

Temperature retrieval with VHF radar using combined techniques

V. Klaus

▶ **To cite this version:**

V. Klaus. Temperature retrieval with VHF radar using combined techniques. Annales Geophysicae, 2008, 26 (12), pp.3805-3817. 10.5194/angeo-26-3805-2008 . meteo-00349028

HAL Id: meteo-00349028

https://meteofrance.hal.science/meteo-00349028

Submitted on 15 Jun 2017

HAL is a multi-disciplinary open access archive for the deposit and dissemination of scientific research documents, whether they are published or not. The documents may come from teaching and research institutions in France or abroad, or from public or private research centers.

L'archive ouverte pluridisciplinaire **HAL**, est destinée au dépôt et à la diffusion de documents scientifiques de niveau recherche, publiés ou non, émanant des établissements d'enseignement et de recherche français ou étrangers, des laboratoires publics ou privés.

Ann. Geophys., 26, 3805–3817, 2008
www.ann-geophys.net/26/3805/2008/
© European Geosciences Union 2008

Annales Geophysicae

Temperature retrieval with VHF radar using combined techniques

V. Klaus

Météo-France, CNRM, 42, avenue Gaspard Coriolis, 31057 Toulouse Cedex, France

Received: 1 October 2007 – Revised: 17 July 2008 – Accepted: 2 September 2008 – Published: 28 November 2008

Abstract. The purpose of this study is to evaluate the practical contribution of a VHF radar to high time resolution automatic temperature profiling both for research and operational applications in the frame of an integrated system of ground-based remote-sensing instruments. Based on the most prominent results already mentioned about this instrumentation, different techniques, related to the temperature data retrieval, are experimentally tested and documented using the INSU/Meteo 45 MHz wind profiler operating at CNRM/Toulouse or during cooperative campaigns. In parallel to the self-sufficient Radio Acoustic Sounding System (RASS), other approaches, using the Brunt-Vaisala frequency measurements, allow an extension of height coverage up to the higher troposphere and the tropopause. As only temperature gradients can be measured by this way, complementary data from other instruments are desirable. This makes it particularly fitted to an integrated remote-sensing system operating from the ground combining wind profilers with GPS, radiometers, lidar ceilometers and sodars.

Keywords. Atmospheric composition and structure (Pressure, density, and temperature; Instruments and techniques) – Meteorology and atmospheric dynamics (Mesoscale meteorology)

1 Introduction

The Radio Acoustic Sounding System (RASS) capabilities to measure virtual temperature profiles using a wind profiler have already been widely attested (Adachi et al., 1993; Angevine et al., 1994; May et al., 1989; Peters, 2000; Klaus et al. 1998). This technology, involving acoustic transmission in the atmosphere combined with an UHF or a VHF radar, is potentially one of the most promising tools for an automated continuous temperature profiling due to its accuracy and efficiency in all weather conditions. This technology has still some important caveats, in particular, the noise pollution and the height coverage limitation. Both theoretical studies and practical observations have been conducted with the RASS in order to evaluate the range coverage and to reduce noise pollution.

To complement the temperature profile above the range covered by the RASS, other possibilities can be exploited with VHF radars by evaluating the Brunt-Väisälä frequency (B-V).

Provided the horizontal wind is not too strong, the most direct way to deduce B-V frequency with a wind profiler is by measuring the variations of the vertical wind velocity (W) at high time resolution of about 1 min. As has already been attested (Ecklund et al., 1985; Röttger, 1985; Revathy et al., 1996), the spectral representation of these variations generally show a peak corresponding to B-V and enable an easy detection of this parameter.

Another possibility of B-V frequency retrieval, which is restricted to altitudes where humidity is negligible, consists in extracting these data directly from the echo spectral power. The dry term of the refractive index gradient M is calculated from the signal-to-noise ratio of the radar (VanZandt et al., 1978; Gage and Balsley, 1980) and temperature is deduced from the general equation relating M to atmospheric parameters.

In order to evaluate the practical capabilities and limits of these techniques, tests have been conducted with the INSU/Météo 45 MHz instrument, either at CNRM/Toulouse or during the Mesoscale Alpine Project (MAP) cooperative campaign in Italy in 1999.

2 Temperature retrieval with the RASS technique

UHF and VHF radars are mainly designed for measuring wind profiles in all weather conditions, including precipitations, as the rain drops are good tracers of horizontal wind.

Correspondence to: V. Klaus
(vladislav.klaus@meteo.fr)

Published by Copernicus Publications on behalf of the European Geosciences Union.

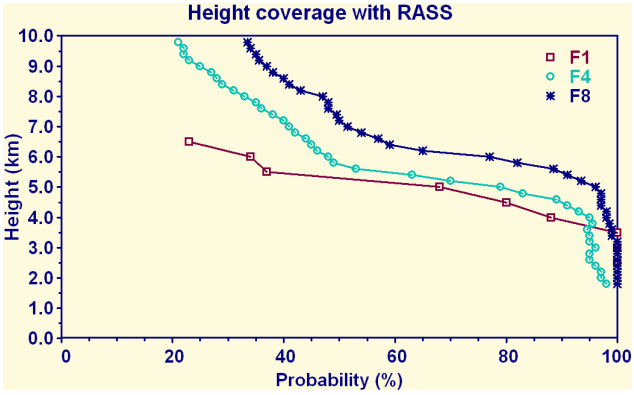


Fig. 1. Experimental results of monthly height coverage with central sources alone (F1) and simulation data using distribution patterns of 4 acoustic sources. at 30 m from the antenna network centre (F4). and 8 sources at 30 m and 60 m from the centre (F8).

As per the Bragg condition, they are sensitive to refractive index variations occurring within the scale of half the radar wavelength. As observed by VanZandt (1983), due to existence of a persistent background of turbulence in the troposphere, clear air echoes from VHF radars are detected in every range gate even with a resolution as small as 150 m. This is no more true above 16 km height where gaps may appear in some range gates. These turbulent layers being advected by the wind, the mean wind vector is easily obtained using several beam directions of the radar.

The RASS technique, already available as an operational option on several manufactured UHF instruments, consists in sending acoustic waves in the atmosphere at approximately half the wavelength of the radar (Peters et al., 1983; May et al., 1990). The acoustic waves produce refractive index perturbations easily perceived by the wind profiler. Their speed calculated by Doppler effect is directly related to the square root of the virtual temperature. By this way, virtual temperature profile is obtained up to the point at which the acoustically induced signal is too weak or has been shifted out the radar sensing volume by the horizontal wind.

Two main points must be underlined at this step: The height coverage limitation, which may need complementary devices, and the acoustic pollution, which may hinder its practical application.

2.1 Range coverage with RASS

The range coverage is limited in height if no advanced and expensive techniques, such as the beam ray tracing, is implemented to track the acoustic wave advected by the horizontal wind (Matuura et al., 1986). Both theoretical studies and practical observations, using the 45 MHz radar at CNRM/Toulouse, have already shown that the probability to get RASS echoes sharply decreases above 6 km height (Klaus et al., 2002). Slight improvement may still be obtained with a larger number of sources distributed around the radar antennas taking also account of the general climatology of the area, but there is no prospect of reaching the tropopause with a low cost technology and ordinary stratotropospheric (ST) radar. As shown in Fig. 1, using 8 acoustic sources distributed at 30 and 60 m from the radar antenna centre instead of a single one, may increase height coverage by about 1 km allowing 6 km altitude to be reached in 50% of cases at least. This may have practical significance for operational system focussed on the lower troposphere.

2.2 Noise pollution with RASS

The second point also deserves particular attention as horizontal noise pollution may hinder practical applications around urban areas where these measurements may be highly required, for example for chemical pollution tracking. With VHF radars, the problem is even somewhat harder as the acoustic frequency needed for RASS is located in the lower audible range at about 80 to 100 Hz, which means weaker attenuation in the atmosphere and a subjectively greater disturbance to the ear. This nuisance may also be enhanced by the low-frequency vibrations of the acoustic transmitter mechanical structure. Contrarily to electromagnetic waves, acoustic signals cannot be easily directed in a narrow beam without an important technical implementation, which a low cost system cannot afford.

The basic acoustic source was a loudspeaker with a galvanized iron elbow directing the signal to the zenith (Fig. 2a). Then several attempts were made to minimize the horizontal noise. They included respectively a soundproof box, a PVC elbow and a one-meter long PVC cylinder extension fixed to the elbow (Pénetier, 2001). While the soundproof box did not bring much improvement, the PVC pipe with its extension attenuated the noise at ground level by 6 dB compared to the mere iron elbow. This solution was finally adopted due to its performance and the implementation convenience (Fig. 2b).

Further improvement was made possible by distributing the sources in an acoustic half-wave-length array of at least 4 identical sources. This very simple principle is already exploited for the coaxial collinear antenna network of the VHF radar in order to focus the signal beam near the vertical. At CNRM/Toulouse, the radar antenna is located in the experimental area at about 300 m from office buildings of the Research Centre (CNRM) and the Meteorological School (ENM). Consequently, stress had been laid on minimizing the pollution in the direction of those edifices.

When using a single acoustic transmitter at the centre of the antenna array, the noise is logically evenly distributed around the source. With a 115 dB acoustic power at 1 m above the horn (equivalent to a power-hammer at the threshold of pain), the horizontal disturbance at the building entrance is between 65 and 70 dB, which corresponds to a noisy conversation, at the limit of fatigue. In spite of being largely



Fig. 2a. The initial acoustic source for RASS.



Fig. 2b. Same as Fig. 2a by replacing the iron elbow by a PVC one and 1-m extension allowing 6 dB attenuation at the ground level.

below the legal threshold requiring protection (85 dB), the sound is still too noisy for being ignored. By using a network of 4 loudspeakers, distant from each other by about half-the acoustic wavelength, the noise can be reduced to no more than 60 dB, equivalent to the standard level of a busy street, which during the day is hidden in any way due to a near-by highway.

The sources are supposed to transmit in a frequency range of 80 to 100 Hz, which is located typically 2 octaves below "middle C" of a piano at the end of the second octave from the left. Inside this range, all the frequencies do not propagate exactly according to the same pattern, because of the interference of the waves generated in phase by the four distant acoustic sources. Consequently, at any point, the transmitted power vis frequency is not exactly uniform. Figure 3 shows examples of acoustic wave horizontal propagation according to the number and distribution of the loudspeakers. For the calculation, only the maximum has been retained, which is closest to the reality perceived by the human ear. We may also notice that in some other directions, by compensation, the noise is considerably increased. Consequently, due consideration should be paid when installing such system near an inhabited area as the results may show large variations even with a slight shifting.

As the CNRM and ENM buildings are not distributed along a simple geometric pattern, only empirical method of sources location was used with the simulation software in order to minimize the noise in these two directions. In this particular situation, 4 properly distributed acoustic sources could significantly reduce the horizontal nuisance. In any other building configuration, the same kind of adjustment should be made according to the number of available sources and the available area.

3 Temperature retrieval using the Brunt-Väisälä (N) evaluation

3.1 Extracting temperature from N

To complement the temperature profile above the range covered by the RASS, other possibilities can be exploited with VHF radars by evaluating first the Brunt-Väisälä (B-V) frequency (N) This parameter can be obtained using two quite different techniques, which are described respectively in Sects. 3.2 and 3.3. First, we need to establish the way of getting temperature profiles from N. N is expressed as:

$$N^2 = \frac{g}{T}\left(\frac{dT}{dz} + \Gamma\right) = \frac{g}{\theta}\frac{d\theta}{dz} = g\left(\frac{d\,\ln\theta}{dz}\right) \quad (1)$$

where g is the gravity acceleration (9.8 m s^{-2}), T is the temperature, z is the height, Γ is the dry adiabatic lapse rate (around 9.76 K/km), and θ is the potential temperature.

Practically, for a standard atmosphere, Eq. (1) shows that N^2 is around 0.0001 rad^2/s^2 in the troposphere where $dT/dz \approx -6.5$ K/km, and 0.0004 rad^2/s^2 in the stratosphere where dT/dz is close to zero. But of courses, important variations may occur, mostly in the troposphere.

In the case of an ideal atmosphere, Γ can be written as:

$$\Gamma = g/c_p \quad (2)$$

c_p being the specific heat of a mixture of dry air and water vapour considered as ideal gases. It can be written in the atmosphere (Gill, 1982):

$$c_p = 1004.6(1 + 0.8375q)\ \mathrm{J\,kg^{-1}\,K^{-1}} \quad (3)$$

where q is the specific humidity.

Thus, we obtain:

$$\Gamma\,(q) = \frac{9.755 \times 10^{-3}}{1 + 0.8375q} \quad (4)$$

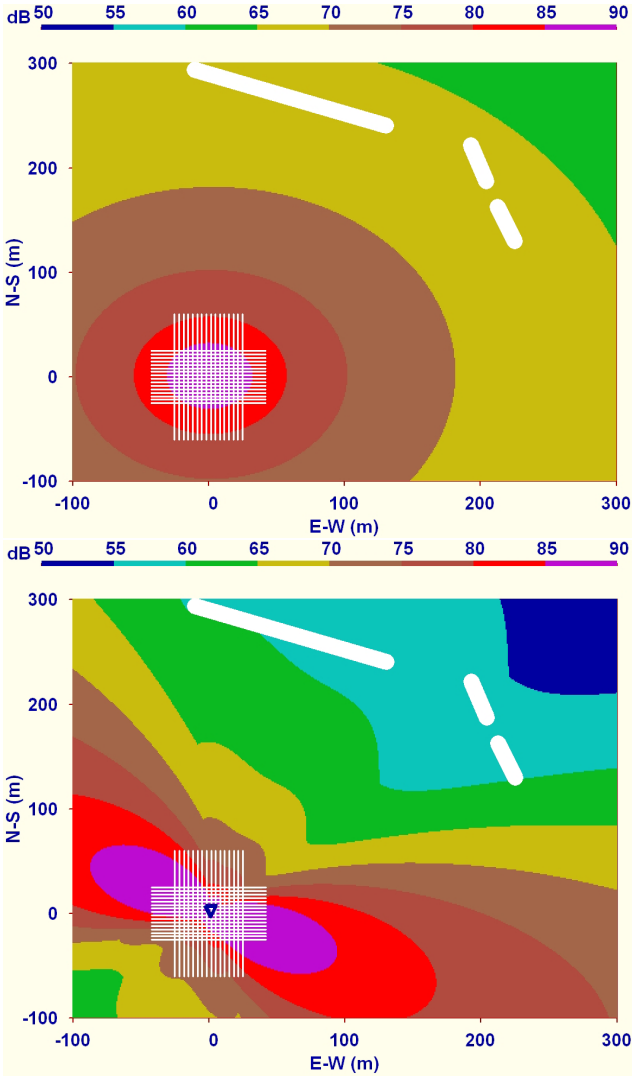


Fig. 3. Horizontal noise pollution with acoustic transmitters at CNRM/Toulouse installed in the centre of the 45 MHz radar antenna (grid) near the Météo-France buildings (white lines). **(a)** Single transmitter, **(b)** 4 transmitters located respectively at the coordinates (0,0), (1.4,1.13), (0.4, 1.75), and (1.8,3.12) relatively to the antenna grid center.

The influence of humidity may not be completely negligible in hot and humid lower troposphere during the monsoon in tropical regions for instance. A saturated air at 24°C contains about 30 hPa of vapour pressure, which at 800 hPa for example (around 2 km) is equivalent to 23 g/kg of specific humidity. Applied to Eq. (4), this influence shifts the value of Γ by about 2%. Consequently, in most of cases, no significant error may be expected by assuming Γ to be a constant

The atmosphere not being an ideal gas, a more accurate expression for Eq. (1) has been given by Richiardone and Giusti (2001). In the same way as for the humidity effect, this correction will not be considered due to its small influence and the degree of complexity it would involve in further calculations.

Assuming Γ to be a constant, Eq. (1) is easily solved as already described by Revathy et al. (1996).

$$\frac{dT}{dz} - \frac{N^2}{g} T = -\Gamma \tag{5}$$

By putting:

$$I(z) = \frac{\theta(z_0)}{\theta(z)} = \exp\left[-\int_{z_0}^{z} \frac{N^2(z')}{g} dz'\right] \tag{6}$$

we can write:

$$I.\frac{dT}{dz} - \frac{N^2}{g} I\, T = -\Gamma\, I \tag{7}$$

or:

$$I\,\frac{dT}{dz} + T\,\frac{dI}{dz} = \frac{d(T\,I)}{dz} = -\Gamma\, I \tag{8}$$

which finally gives by integration:

$$T(z) = \frac{1}{I(z)}\left[I(z_0)\; T(z_0) - \Gamma \int_{z_0}^{z} I(z')\; dz'\right] \tag{9}$$

or its equivalent in term of potential temperature:

$$T(z) = \theta(z)\left[\frac{T(z_0)}{\theta(z_0)} - \Gamma \int_{z_0}^{z} \frac{1}{\theta(z')} dz'\right] \tag{10}$$

Due to the presence of the integral in the expression of Eq. (9), an initial value of $T(z_0)$ at a given range gate z_0 is needed to calculate the T profile. It can be obtained for example from the RASS measurements in the lower ranges. If humidity data are available or at least estimated, Γ can further be fine-tuned, but it has been shown that no much effect is produced on final results. However, when using RASS virtual temperature (Tv) measurements, they will help to provide more rigorously the initial value $T(z_0)$ from $Tv(z_0)$.

As previously mentioned, N can be extracted from radar data by two different techniques using respectively the echo power in the case humidity is negligible and the vertical wind variations. They will be described in the following chapters.

Figure 4 shows some examples of B-V obtained respectively by the signal power (VHF_SP) and the vertical wind spectrum methods (VHF_WS). It is interesting to note that both can be efficient in providing this parameter. VHF_WS tends to smooth the data in the troposphere, while VHF_SP is much more sensitive at this level.

3.2 Temperature retrieval with the echo power technique

3.2.1 Theoretical background

A possibility, which is restricted to altitudes where humidity is negligible, consists in extracting B-V data from the echo

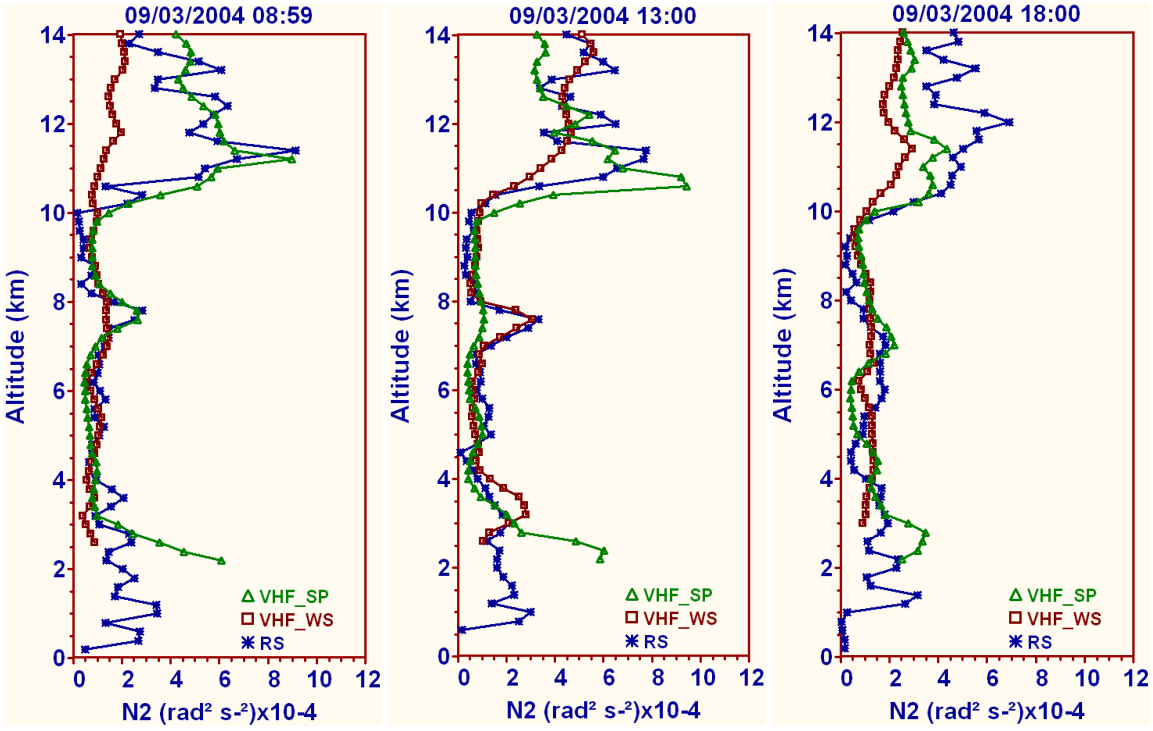


Fig. 4. Comparison of N^2 between radio soundings (RS) and VHF radar (VHF) using respectively the signal power (VHF_SP) and the vertical wind spectrum (VHF_WS) method.

spectral power of the ST radar as has already been shown by Hooper et al. (2004). To this purpose, the dry term of the refractive index gradient M is first estimated from the radar data through the expression of the refractivity turbulence structure constant C_n^2 (VanZand et al., 1978).

$$C_n^2 = 2.8 L_0^{4/3} M^2 = \frac{\eta}{0.38} \lambda^{1/3} \tag{11}$$

where L_0 is the outer scale length of the turbulence spectrum, η is the radar reflectivity extracted from the echo power intensity (VanZandt et al., 1978; Gage and Balsley, 1980), and λ is the radar wavelength..

M is directly expressed from radar reflectivity η as:

$$|M| = 0.97 L_0^{-2/3} \lambda^{1/6} \eta^{1/2} \tag{12}$$

Besides, M is related to atmospheric parameters as follows:

$$M = -77.6 \times 10^{-6} \frac{P}{T} \left[\frac{N^2}{g} \left(1 + 15600 \frac{q}{T} \right) - \frac{7800}{T} \frac{dq}{dz} \right] \tag{13}$$

where P is the atmospheric pressure (hPa), T is the temperature (K), g is the acceleration of gravity ($\mathrm{m\,s^{-2}}$), q is the specific humidity (g/g), and z is the altitude. When humidity is negligible, we simply have the dry contribution M_D:

$$M_D \approx -77.6 \times 10^{-6} \frac{P}{T} \frac{N^2}{g} \tag{14}$$

Then, N^2 is deduced from the combination of Eqs. (12) and (14):

$$N^2 = 1.25 \times 10^4 \, g \frac{T}{P} \, L_0^{-2/3} \lambda^{1/6} \eta^{1/2} \tag{15}$$

3.2.2 Practical implementation

η may not be correctly estimated due to difficulties to calibrate the radar properly and the possible fluctuations of the radar performances with time. If accurate results should be sought, the daily variations of the cosmic noise must also be considered in order to evaluate the noise level to be substracted from the signal-to-noise ratio (Campistron et al., 2001). At this step, we simply consider that η is only estimated through a multiplication constant to be evaluated from validation with radio soundings. Practically, comparisons of M profiles calculated both from the radiosonde data and the profiler on preliminary campaigns are very useful.

As discussed in Hooper et al. (2004), L_0 may not be a constant, with respect both to time and altitude. This has led to an alternative form of the expression of the radar return signal power (for example Gage et al., 1980). This assumption quoted by Hooper and Thomas (1998) where L_0 may depend on N^2 resulting in η proportional to N^4 has given correct results concerning humidity retrieval (Tsuda et al., 2001; Klaus et al., 2006).

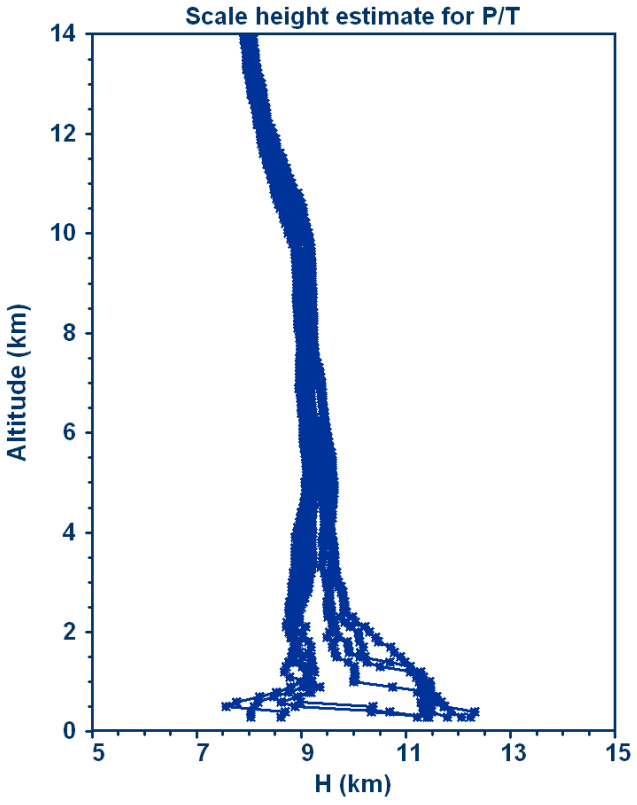


Fig. 5a. Scale height relative to the ratio P/T computed from a series of radiosoundings at CNRM/Toulouse.

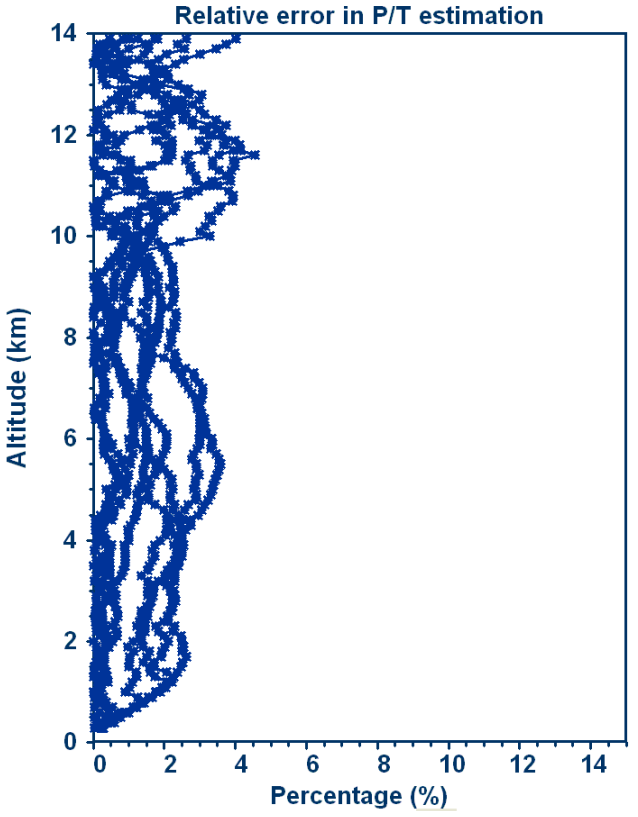


Fig. 5b. Relative error involved by replacing P/T values by $P_0/T_0 \exp[-(z-z_0)/H]$ with H equal to 9000 m below 9 km height with a linear decrease of 1 km per 3.5 km above this height.

However, a number of radiosonde comparisons made at different times and locations has confirmed the proportionality of M^2 with the radar reflectivity η (Röttger, 1979; Tsuda et al., 1988; Hocking and Mu, 1997; Hooper and Thomas, 1998; Low et al., 1998). Local tests at CNRM/Toulouse have confirmed these results showing that the best temperature results were obtained with L_0 considered as constant, but taking a different value from the troposphere to the stratosphere. Consequently, the knowledge of the tropopause height appears to be a valuable complement for this study.

The problem to find the exact value of L_0 is minimized by the fact empirical calibration is already made to evaluate η from radar signal to noise and only a global constant including both calibration value and L_0 is required to apply the method.

Consequently, in Eq. (15) constant parameters can be combined under:

$$K = 1.25 \times 10^4 \, g \, L_0^{-2/3} \, \lambda^{1/3} \tag{16}$$

where K is evaluated once for all with a possible variation between the troposphere and the stratosphere.

This finally leads to:

$$N^2 = K \frac{T}{P} \, \eta^{1/2} \tag{17}$$

Equation (17) contains pressure data, which may not be available in a completely independent remote sensing system. One direct way is to use the previous estimations from the model forecasting, as small variations of P have little influence on the general accuracy of the method.

Another way is to replace P/T, which is proportional to the air density, by an expression depending only on ground measurements $\frac{P}{T} = \frac{P_0}{T_0} \exp\left(-(z-z_0)/\overline{H}\right)$ (Hooper et al., 2004), where P_0 and T_0 are the pressure and temperature respectively at ground level z_0, and $\overline{H}$ is the mean scale height across the whole altitude range. Here $\overline{H}$ should not be confused with the more traditional scale height used for computing pressure profile. The general profile of $\overline{H}$, measured from a series of radiosoundings at CNRM/Toulouse, is around 9000 m the troposphere with a slight decrease of about 1 km per 3.5 km above this level (Fig. 5a). Larger variations occur below 5 km, but without effect on the relative error due to compensation by larger values of P and smaller altitude z. This stable behaviour above this height allows a simple linear modelization of $\overline{H}$ for further studies. Figure 5b shows that relative error involved by this formulation is below 4%, which allows to keep same the differential equation (Eq. 5) for extracting the temperature profile.

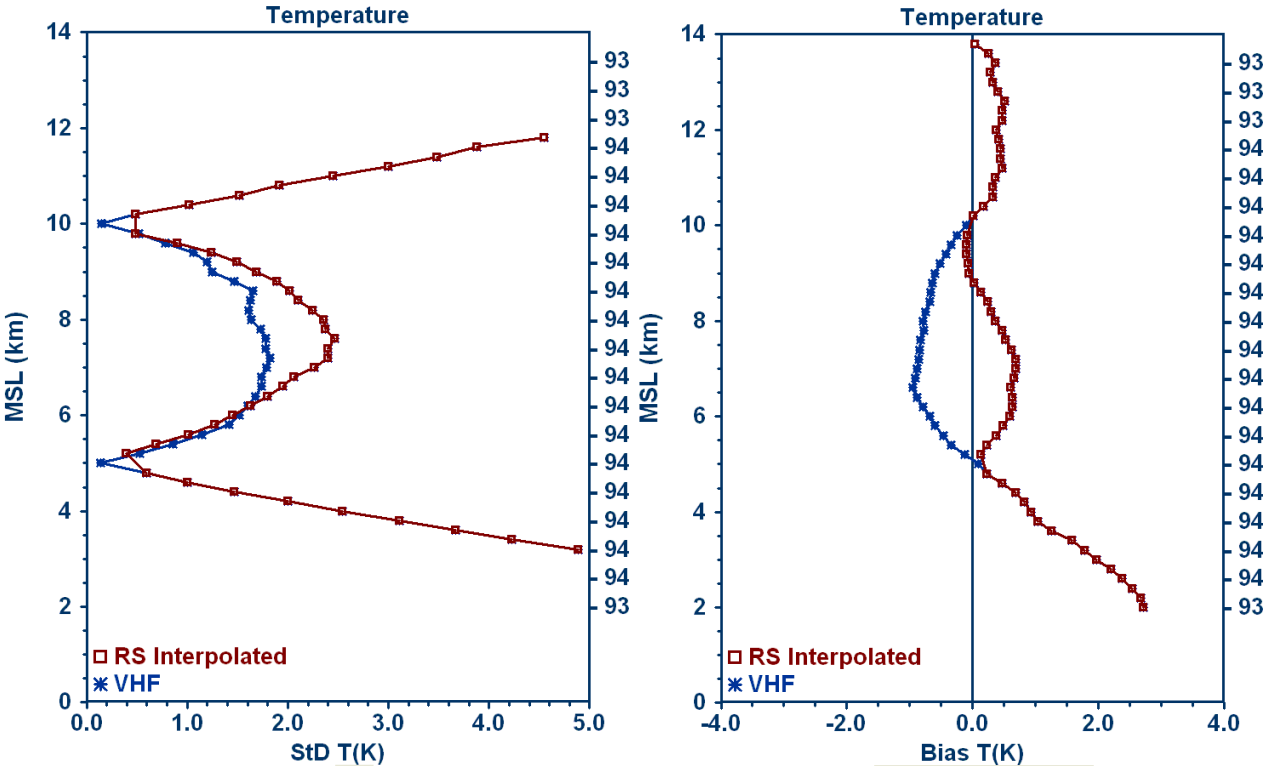


Fig. 6. Standard deviation **(a)** and bias **(b)** between radiosonde (RS) temperature measurements and respectively VHF radar temperature computed with the echo power technique (VHF) with reference values between 5 and 10 km, and interpolated temperature data from RS between 5 and 10 km. The column on the right indicates the number of comparisons used for the statistics.

Equation (15) can be expressed as follows:

$$N^2 = K\,\rho_0^{-1} \exp\left[\frac{z}{H}\right] \eta^{1/2} \tag{18}$$

Then T profile is calculated in the same way as with the previous method with a second variable K to solve the system of Eqs. (10) and (16). Either, this value is estimated from preliminary radio soundings and then adopted for the whole measurement campaign, or calculation is made for each profile in a two-variable (K and T) resolution equation, in which case, two reference T points are needed to solve the problem. In practical application, the second reference point can be provided for example by commercial jet liners at upper height as already implemented in real time by the Aircraft Meteorological Data Relay (AMDAR) System. As reported by the EUMETNET (2004), the data are available through Global Telecommunication System in less than 30 min in 80% of cases. Radiometric profiler with integrated data over a larger range can be a substitute. Solution is then brought in by numeric method where K is adjusted by successive dichotomy until agreement is reached at both reference points.

3.2.3 Limitations/caveats

The main limitation of this technique in the troposphere is of course the presence of humidity, because the radar signal return power provides $|M|$ (Eq. 12), while only the dry component M_D is needed for the B-V evaluation (Eq. 14). This influence has been discussed in Hooper et al. (2004) from comparisons with 221 radiosondes, showing great discrepancies below 4 km altitude. This is confirmed by the measurements made at CNRM/Toulouse (Fig. 4). It must also be noted that for a given $|M/M_D|$ ratio, the error will be all the more greater as N is important, so the impact will not be same if its value is 0.02 rad s^{-1} or 0.005 rad s^{-1}.

It has also been observed that precipitation may seriously hinder the data quality, first by introducing a spurious echo, and second by removing from the turbulence echo a part of the small-scale refractivity structure related to fluctuations in humidity (Chu and Liu, 1994; Vaugham and Worthington, 2000).

In the frame of this study, the first 5/6 kms are supposed to be covered by the RASS, so that a part of these limitations would not apply above this range, at least in temperate regions.

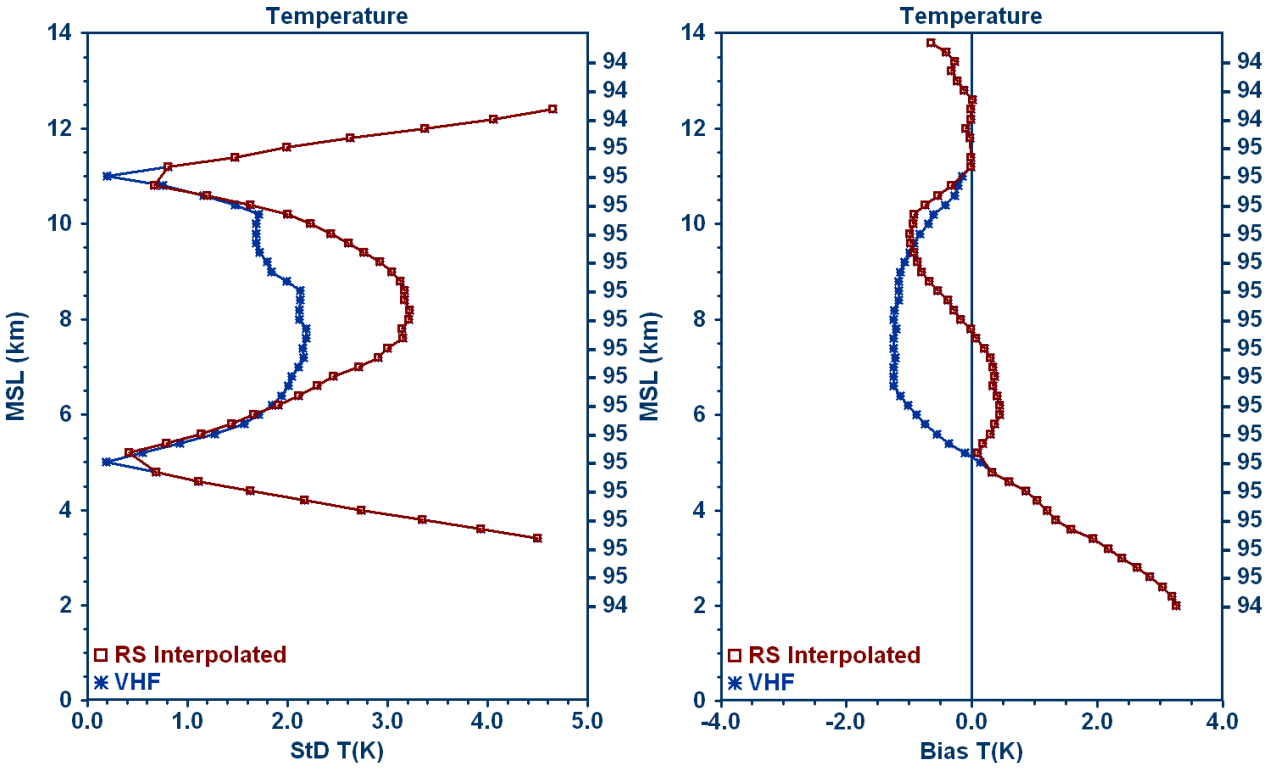


Fig. 7. Same as Fig. 6 with reference values between 5 and 11 km.

We have also seen that the mean scale height is constant in the range 5 to 10 km in which case it is possible to express the P/T ratio with sufficient accuracy based only on ground measurements. Above the tropopause, $\overline{H}$ can be estimated as a function of altitude.

3.2.4 Experimental results

The two-month Mesoscale Alpine Project (MAP) Campaign in the region of Milan (Italy) was used to test this technique (Bougeault et al., 2001). A large number of controlled VHF radar measurements were available and completed with daily radio soundings.

Here we simulated the improvement to be expected when T is measured between 2 levels in the troposphere and near the tropopause respectively by the RASS (5 km) and a jet liner (10, 11, and 12 km, respectively). For each range gate, the standard deviation (StD) and bias of the difference between the radiosonde, and radar-derived values were computed. StD is reduced to about 2 K with the couple 5–10 km (Fig. 6) and 5–11 km (Fig. 7). The results get degraded with the couple 5–12 km (Fig. 8), however this may not be too detrimental for a practical application of the method as most jet liners fly below this altitude. The same statistics have been calculated by replacing the radar-derived values by a simple interpolation of T between the two reference levels. StD becomes closer to or above 3 K. It must also be noted that outside the range connecting the two levels, the method is no more accurate, so that it may not be applicable in the stratosphere if temperature data are available only up to 10 or 11 km height.

3.3 Temperature retrieval with the vertical wind variation technique

3.3.1 Theoretical background

Provided the horizontal wind is not too strong, the most direct way to deduce N with a wind profiler is by using the vertical wind velocity (W) spectra at high time resolution (around 1 min). As has already been attested (Ecklund et al., 1985; Röttger, 1985), the spectra show the "B-V cut off" with a spectral peak at the B-V frequency characterised by a steeper decrease on the side of higher frequencies. This has been confirmed with the VHF radar at CNRM/Toulouse and validated by radio soundings (RS) (Fig. 9). From then, T profiles can be deduced as has already be demonstrated by Revathy et al. (1996) and Mohan et al. (2001).

3.3.2 Practical implementation

The first step is to check the accuracy of the vertical velocity measurement. This is not always an easy task as the

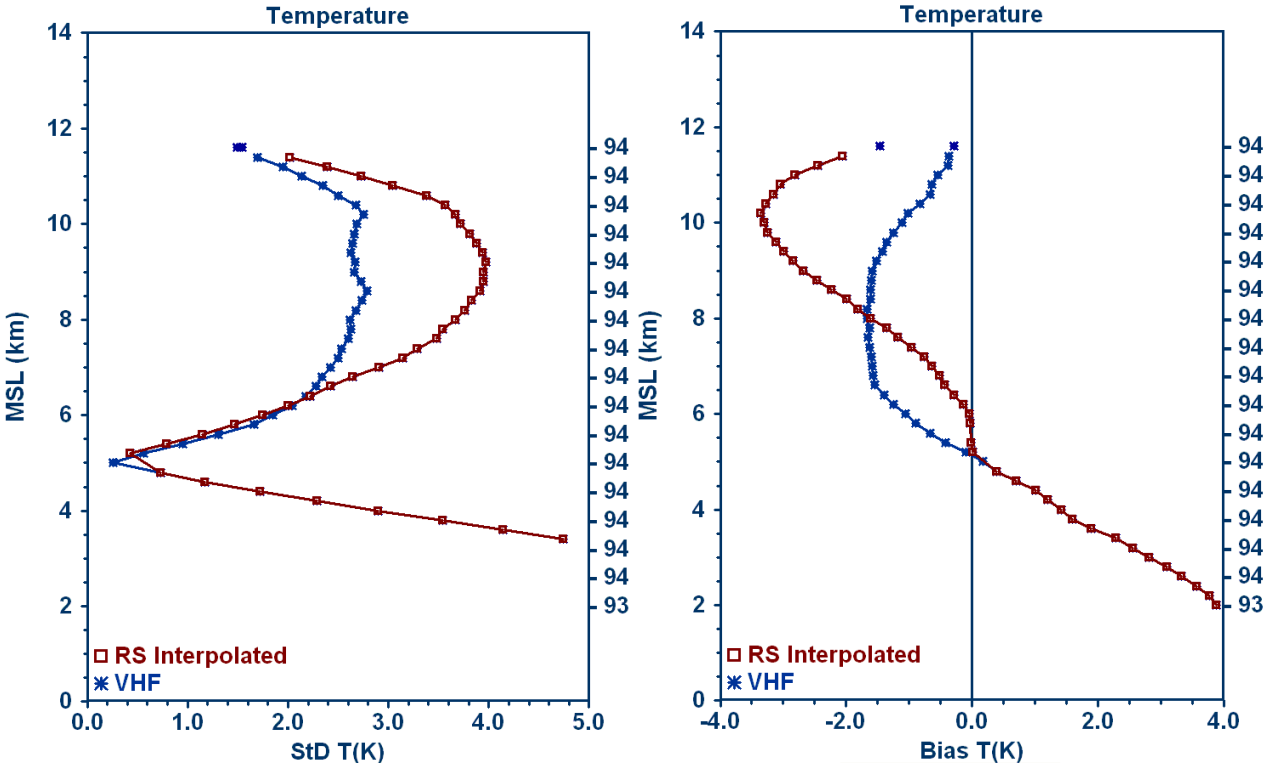


Fig. 8. Same as Fig. 7 with reference values between 5 and 11 km.

vertical velocity to be calculated may be polluted by the ground clutter or near-zero frequency noise. A good separation could be obtained only after further coherent integration, i.e. a spectral zooming near zero frequency, and a zero padding, which increases the spectral resolution. A more advanced method consists in filtering the time series using wavelet packet decomposition as described by Jordan and Lataitis (1997). The opportunity of such filtering has been attested at CNRM/Toulouse (Klaus and Chérel, 2003).

Figure 10 gives an example of vertical wind velocity spectra. A signal corresponding to the B-V frequency is easily observed at all range gates with a typical slope on the right side towards higher frequencies.

3.3.3 Limitations/caveats

This technique cannot be applied in all meteorological conditions. For example for super-adiabatic lapse rates when the B-V frequency become imaginary. Also, during strong horizontal winds, the spectra do no more show a peak followed by a sharp decrease and consequently to accurately locate the B-V peak, as it has been asserted by extended campaigns (Ecklund et al., 1985).

For an automated implementation, it must be stressed that any error or inaccurate location of the peak at a given range gate will have repercussions on all the following altitudes. Consequently, a rigorous checking will be required for its efficient implementation. In order to approach the skill level of the human expert, a fuzzy-logic software will be implemented at CNRM/Toulouse in 2009, in a similar way as was already successfully tested on ST radars for an optimal selection of turbulent peaks on the spectra. (Cornman et al., 1998). This method consists in allotting a table of values, called membership function, for each criterion needed to accept a signal for further processing.

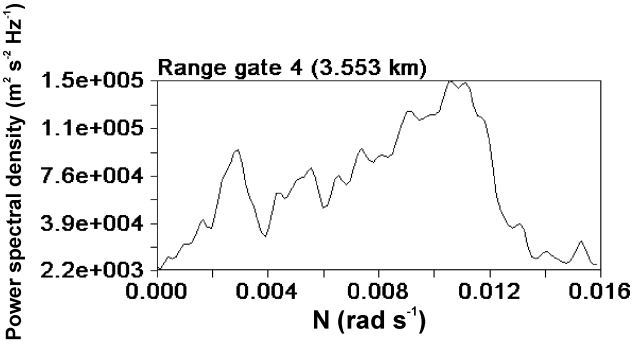


Fig. 9. Example of vertical velocity spectrum obtained with the VHF radar at 3550 m on 26 March 2002 between 12:00 and 12:30 UTC (34 s resolution profiles with zero-padding up to 256 spectral points). The B-V frequency appears as a peak around 0.011 rad s^{-1} corresponding to about 571 s (9 mn 31 s) periodicity.

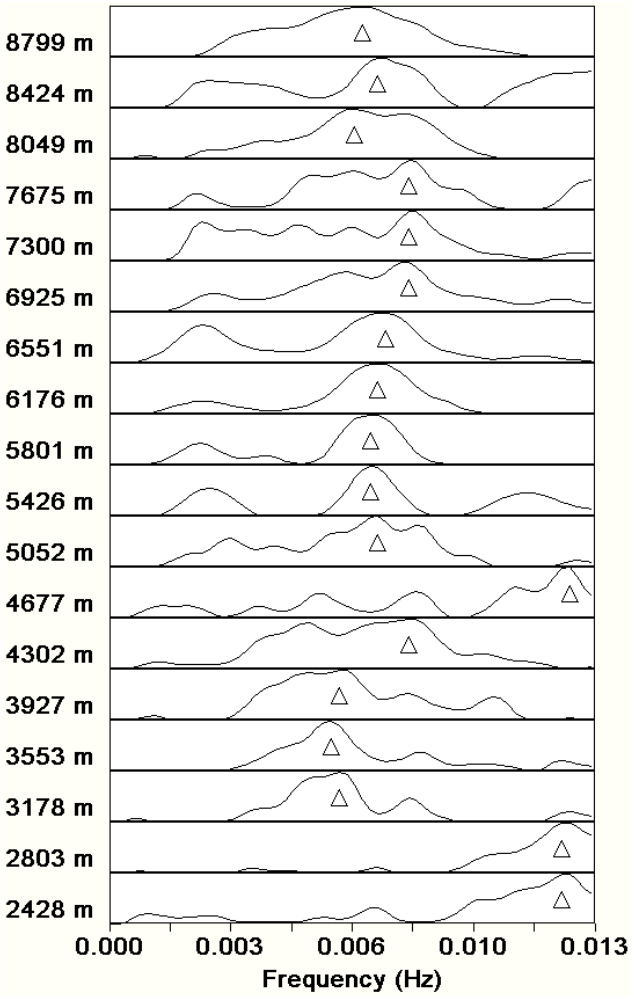


Fig. 10. Vertical wind spectra obtained with the VHF radar on 22 February 2002 between 12:17 and 12:31 UTC (45 s resolution profiles with zero-padding up to 128 spectral points). Peaks are mentioned by triangles.

A number of criteria will be selected at each of the three steps.

- On the raw vertical beam spectra, most of the ground clutter pollution is supposed to have been removed in the preliminary time series filtering. Thus we need to check the presence of a single peak, its detectability above the white noise, and its general form compared to a Gaussian by the skew or 3rd moment evaluation.
- On the time series of vertical velocities. At each range gate, we must check the number of valid points without too many gaps for a proper spectral analysis.
- On the vertical velocity spectra: as shown on Figs. 9 and 10, a non-ambiguous peak must appear, which means that no other concurrent peak is present within several dBs.

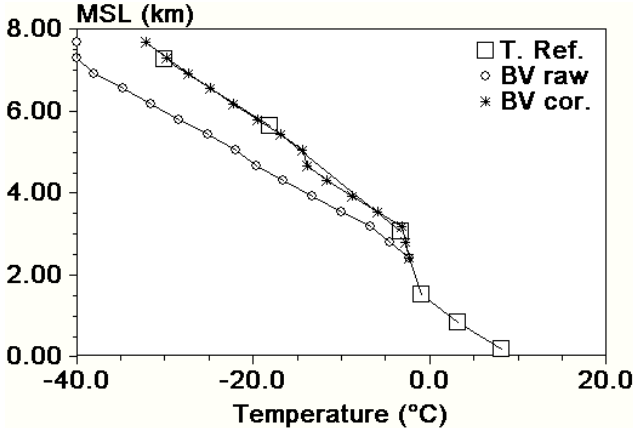


Fig. 11. Temperature profiles obtained from the B-V measurements using peak frequency (BV raw) from Fig. 6, and a factor correction on the frequency (BV cor.), compared to the reference temperature profiles provided by the analysis output from the ECMWF model (T. Ref).

Beside these steps involving vertical velocity data, the horizontal velocity also needs to be checked.

Using the membership function for each of these criteria, we can put a mark on the quality of the measurement. The linear combination of all the values provides a global estimate, which finally indicates if the technique can be applied or not. Tests with experimental data will be needed to define the various parameters related to each membership function and their linear combination.

Contrarily to the previous method, one reference point should theoretically be sufficient for providing T-profile. However, the frequency abscissa of the maximum of the peak is not always a good indicator for temperature retrieval. Figure 11 shows an example when this value must be increased toward the higher frequency base of the peak. Using a global multiplying factor of 1.5 and starting with a reference value at 2400 m provided by the analysis output from the European Centre for Medium Range Weather Forecast (ECMWF) model, we get a much better agreement at 3000, 5600 and 7300 m. A significant gradient variation can even be seen around 3000 m along with an increase of B-V frequency in a small slab at 4000–4500 m which allows a nearly exact alignment of temperature profiles at higher altitudes. This value may change with time.

Experiments with the same type radar in Lannemezan have also shown the necessity to take the right side base of the peak in order to get satisfactory temperature profiles (B. Campistron, personal communication, 2002).

Consequently, for efficient implementation, a second reference point is considered desirable. This will also minimize the effects of any inaccuracy on the peak detection as mentioned above.

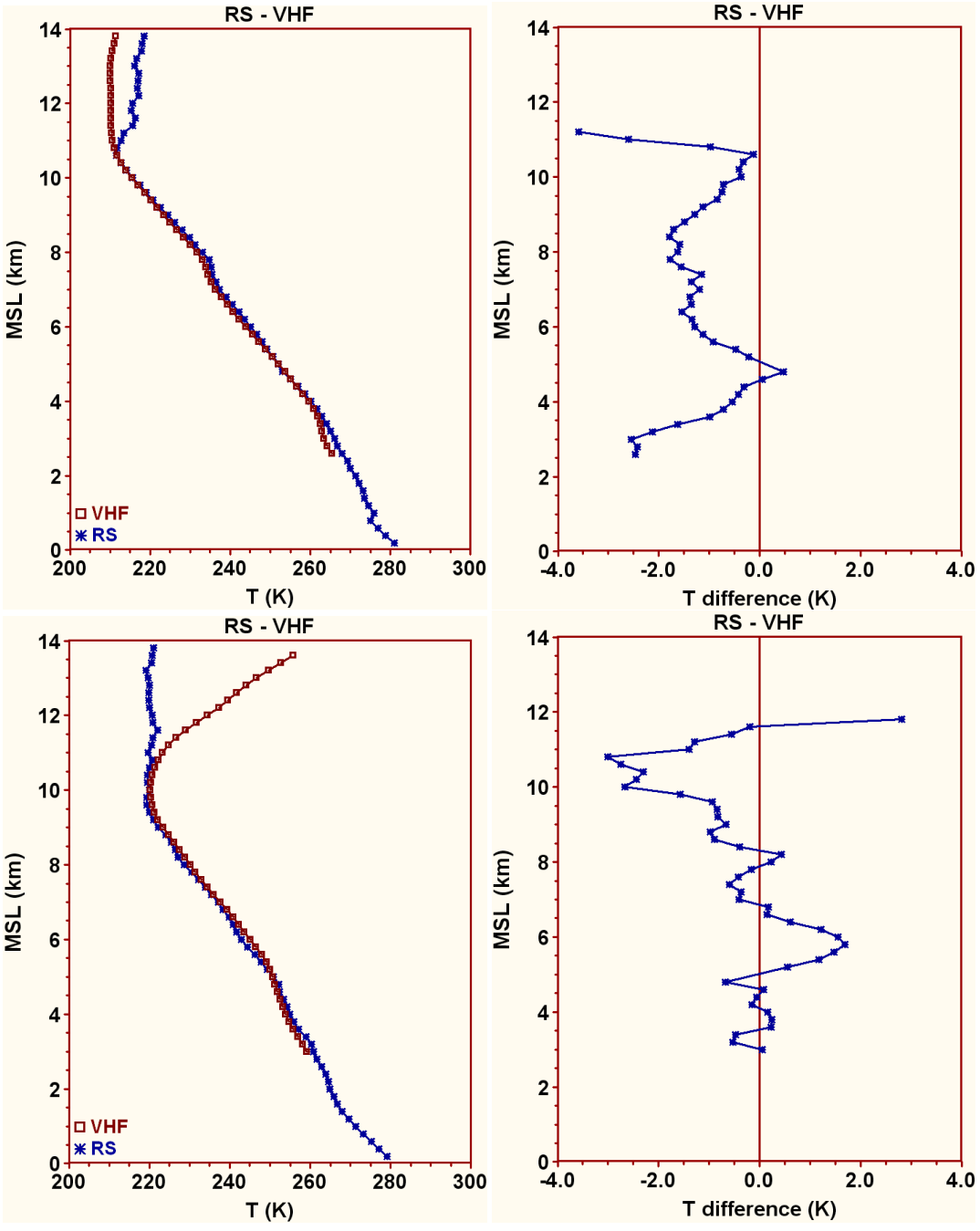


Fig. 12. Comparison of T between radio soundings (RS) and VHF radar (VHF) using the B-V frequency calculation through the vertical speed spectra (Left: Absolute values, right: Temperature differences). The starting point at the 5 km range gate has been extracted from the RS measurements.

3.3.4 Experimental results

With the above considerations, very encouraging results have been obtained with the VHF radar at CNRM/Toulouse compared to 7 radio soundings (RS). As a special configuration of the radar was necessary for continuous vertical profiling during at least 20 min per hour, no data were exploitable from previous cooperative campaigns, which included only regular beam swinging in the vertical and 4 oblique directions in 15 min cycles. This explains much fewer comparison profiles were available as particular measurements had to be made on site to this purpose.

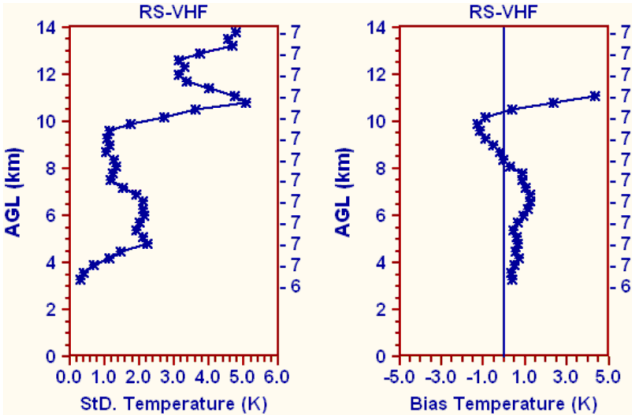


Fig. 13. Standard deviation (left) and bias (right) between temperature profiles provided respectively by radiosonde (RS) and VHF radar (VHF) using the vertical wind spectrum method (VHF_WS) at various range gates. The columns at the right of the figures indicate the number of comparisons used for the statistics.

Figure 12 gives some examples of temperature retrieval using the VHF_WS method with comparisons with radiosonde data. The temperature differences are less than 2 K between 5 and 10 km height.

Statistical results with the VHF_WS have shown a standard deviation between 1 and 2 K up to 10 km (Fig. 13), which represents roughly the tropopause height. Above this level, data are less accurate and could not at this step be taken as reference for an operational exploitation. The may be due essentially to the lack of accuracy involved by the signal attenuation at the upper range gates due to power limitations of the VHF radar (6 kW peak power$\times$4000 m^2 antenna).

4 Conclusion

The RASS technology allows virtual temperature measurements up to 6 km height with a few kW peak power VHF radar using very simple loudspeakers distributed around its antennas. It has also been shown that a proper distribution of the acoustic transmitters may significantly minimize the noise disturbance in selected directions reducing by the way the restriction zone in inhabited areas. Besides, even in the absence of costly ray-tracing techniques, the capabilities of VHF radars in the field of temperature measurement are not limited to the RASS technology and the lower troposphere. Extensions to higher ranges could be made using the Brunt-Väisälä frequency measurements with some restrictions already mentioned.

Either the spectra of the vertical velocities measured at one-minute frequency or directly the echo power from altitudes where humidity is negligible can be exploited to this end. As in both cases differential equations must be solved, complementary temperature data are required. Validations with radiosoundings have shown that accuracy from the vertical velocity spectra analysis may reach 1 to 2 K under the tropopause. With the echo spectral power technique, less than 2 K standard deviation error could also be obtained between two reference altitudes where temperature is known, typically at the top of the RASS profile (5 km) and along the jet liners routes (10–11 km), respectively. Above the tropopause, values are not so good and further studies would be needed before extending furthermore in altitude the methodology.

These techniques are particularly suited to an integrated remote-sensing system including for example a radiometric profiler, a lidar or AMDAR data able to provide complementary information on temperature either at a given level or over a larger range.

Acknowledgements. This study was made possible with the precious help of the technical staff of CNRM/SC/LEM R. Durbe, G. Chérél, and A. Frappier operating the VHF radar with its RASS component either at Meteopole/Toulouse or in Italy during the MAP Experiment. It has also been encouraged by the many fruitful exchanges in the frame of the COST 720 Action, financed by the European Commission, where experts from several European countries dealt with the operational capabilities of ground based integrated remote sensing systems. At Météo-France, the study was also a part of the 2004–2007 GAME prospective plan, supported by the French scientific community.

Topical Editor U.-P. Hoppe thanks two anonymous referees for their help in evaluating this paper.

References

Adachi, T., Tsuda, T., Masuda, Y., Takami, T., Kato, S., and Fukao, S.: Effects of the acoustic and radar pulse length ratio on the accuracy of Radio Acoustic Sounding System (RASS). Temperature measurements with monochromatic acoustic pulses, Radio Sci., 28, 571–583, 1993.

Angevine, W. M., Ecklund, W. L., Carter, D. A., Gage, K. S., and Moran, K. P.: Improved radio acoustic sounding techniques, J. Atmos. Oceanic Technol., 11, Part 1, 42–49, 1994.

Bougeault, P., Binder, P., Buzzi, A., Dirks, R., Houze, R., Kuettner, J., Smith, R. B., Steinacker, R., Volkert, H., et al.: The MAP Special Observing Period, B. Am. Meteorol. Soc., 82, 433–462, 2001.

Campistron, B., Despaux, G., Lothon, M., Klaus, V., Pointin, Y., and Mauprivez, M.: A partial 45 MHz sky temperature map obtained from the observations of five ST radars, Ann. Geophys., 19, 863–871, 2001, http://www.ann-geophys.net/19/863/2001/.

Chu, Y. L. and Lin, C. H.: The severe depletion of turbulent echo power in precipitations observed using the Chung-Li VHF Doppler radar, Radio Sci., 29 1311–1320, 1994.

Cornman, L. B., Goodrich, R. K., Morse, C. S., and Ecklund, W. L.: A Fuzzy Logic Method for Improved Moment Estimation from Doppler Spectra, J. Atmos. Oceanic. Technol., 15(6), 1287–1305, 1998.

Ecklund, W. L., Balsley, B. B., Carter, D. A., Riddle, A. C., Crochet, M., and Garello, R.: Observations of vertical motions in the

troposphere and lower stratosphere using three closely spaced ST radars, Radio Sci., 20, 1196–1206, 1985.

EUMETNET: Quarterly reports of the E-AMDAR Quality Evaluation Centre on AMDAR data, 2003-IV, Report number 17, 28 May 2004.

Furumoto, J., Kurimoto, K., and Tsuda, T.: Continuous Observations of Humidity Profiles with the MU Rada-Rass Combined with GPS and Radiosonde Measurements, J. Atmos. Ocean. Technol., 20, 23–41, 2003.

Furumoto, J.-I., Tsuda, T., and Iwai, S.: Continuous humidity monitoring in a tropical region with the Equatorial Atmosphere Radar, J. Atmos. Oceanic Technol., 23, 538–551, 2006.

Gage, K. S. and Balsley, B. B.: On the scattering and reflection mechanisms contributing to clear air radar echoes from troposphere, stratosphere and mesosphere, Radio Sci., 15, 243–257, 1980.

Gage, K. S., Green, J. L., and Vanzandt, T. E.: Use of Doppler radar for the measurement of atmospheric turbulence parameters from the intensity of clear air echoes, Radio Sci., 15, 407–416, 1980.

Gill, A. E.: Atmosphere-Ocean Dynamics, Academic Press, 662 pp, 1982.

Hocking, W. K. and Mu, P. K. L.: Upper and middle atmospheric kinetic energy dissipation rates from measurements of Cn^2 – Review of theories in-situ investigations, and experimental studies using the Buckland Park atmospheric radar in Australia, J. Atmos. Sol.-Terr. Phys., 59, 1779–1803, 1997.

Hooper, D. A. and Thomas, L.: Complementary criteria for identifying regions of intense atmospheric turbulence using lower VHF radar, J. Atmos. Terr. Phys., 60, 49–61, 1998.

Hooper, D. A., Arvelius, J., and Stebel, K.: Retrieval of atmopheric static stability from MST radar return signal power, Ann. Geophys., 22, 3781–3788, 2004, http://www.ann-geophys.net/22/3781/2004/.

Jacoby-Koaly, S., Campistron, B., Bernard, S., Bénech, B., Ardhuin-Girard, F., Dessens, J., Dupont, E., and Carissimo, B.: Turbulent Dissipation Rate in the Boundary Layer via UHF Wind Profiler Doppler Spectral Width Measurements, Bound.-Lay. Meteorol., 103, 361–389, 2002.

Jordan, J. R. and Lataitis, R. J.: Using wavelet filtering to reduce ground clutter contamination in wind profiler signals, COST-76 Profiler Workshop, Engelbert, Switzerland, 119–122, 1997.

Klaus, V., Aubagnac, J.-P., v. Baelen, J., Chérel, G., Durbe, R., and Frappier, A.: New developments with the INSU/Météo VHF radar at CNRM/Toulouse: RASS, FDI and upgraded processing techniques, Meteor. Zeit., NF7, 355–365, 1998.

Klaus, V., Chérel, G., Goupil, P., and Pénetier, N.: RASS Developments on the VHF Radar at CNRM/Toulouse Height Coverage Optimization, J. Atmos. Ocean. Technol., 19, 967–979, 2002.

Klaus, V. and Chérel, G.: Wavelet packets as a tool for profiler data filtering, 6th International Symposium on Tropospheric Profiling: Needs and Technology, 14–20 September 2003, Leipzig, Germany, 94–96, 2003.

Klaus, V., Bianco, L., Gaffard, C., and Hewison, T.: Combining UHF radar wind profiler and microwave radiometer for the estimation of atmospheric humidity profiles, Meteor. Zeit., 15, 87–97, 2006.

Low, D. J., Reid, I. M., Vincent, R. A., and May, P. T.: Predicting VHF wind profiler temperature from (p,T,q) soundings, 8th Workshop on Technical and Scientific Aspects of MST Radar, Bangalore, India, Step Handbook, 294–297, 1998.

Matuura, N., Masuda, Y., Inuki, H., Kato, S., Fukao, S., Sato, T., and Tsuda, T.: Radio acoustic measurement of temperature profile in the troposphere and stratosphere, Nature, 323, 426–428, 1986.

May, P. T., Moran, K. P., and Strauch, R. G.: The accuracy of RASS temperature measurements, Appl. Meteorol., 28, 1329–1335, 1989.

May, P. T., Strauch, R. G., Moran, K. P., and Ecklund, W. L.: temperature soundings by RASS with wind profiler radars, IEEE Trans. Geosci. Rem. Sens., 28, 19–28, 1990.

Mohan, K., Rao, D. N., Rao, T. N., and Raghavan, S.: Estimation of temperature and humidity from MST radar observations, Ann. Geophys., 19, 855–861, 2001, http://www.ann-geophys.net/19/855/2001/.

Pénetier, N.: Etude et limitation des nuisances sonores générées par le système de télédétection R.A.S.S., Note de travail de l'ENM, 785, 99 pp, 2001.

Peters, G., Timmerman, H., and Hinzpeter, H.: Temperature sounding in the planetary boundary layer by RASS – System analysis and results, Int. J. Rem. Sens., 4, 49–63, 1983.

Peters, G.: RASS, present state, prospects, and open questions, 5th International Symposium on Tropospheric Profiling, Adelaide, Australia, 231–233, 2000.

Revathy, K., Nair, S. R. P., and Murthy, B. V. K.: Deduction of temperature profile from MST radar observations of vertical wind, Geophys. Res. Lett., 23, 285–288, 1996.

Richiardone, R. and Giusti, F.: On the Stability Criterion in a Saturated Atmosphere, J. Atmos. Sci., 58, 2013–2017, 2001.

Rottger, J.: VHF radar observations of a frontal passage, J. Appl. Meteorol., 18, 85–91, 1979.

Röttger, J.: Determination of the Brunt-Vaisala frequency from vertical velocity spectra, Handbook for MAP, 20, 168–172, 1985.

Tsuda, T., May, P. T., Sato, T., Kato, S., and Fukao, S.: Simultaneous observations of reflection echoes and refractive index gradient in the troposphere and lower stratosphere, Radio Sci., 23, 655–665, 1988.

Tsuda, T., Miyamoto, M., and Furumoto, J.: Estimation of a Humidity Profile Using Turbulence Echo Characteristics, J. Atmos. Ocean. Technol., 18, 1214–1222, 2001.

VanZandt, T. E., Green, J. L., Gage, K. S., and Clark, W. L.: Vertical profiles of refractivity turbulence structure constant: Comparison of observation by the Sunset radar with a new theoretical model, Radio Sci., 13, 819–829, 1978.

VanZandt: Existence of a permanent background of turbulence, Handbook for MAP, 9, 256–261, 1983.

Vaugham, G. and Worthington, R. M.: Effects of humidity and precipitation on VHF radar vertical-beam echoes, Radio Sci., 35, 1389–1398, 2000.

Warnock, J. M. and VanZandt, T. E.: A statistical model to estimate the refractivity turbulence structure constant Cn^2 in the free atmosphere, NOAA Technical Memorandum, ERL AL-10, 176, 1985.